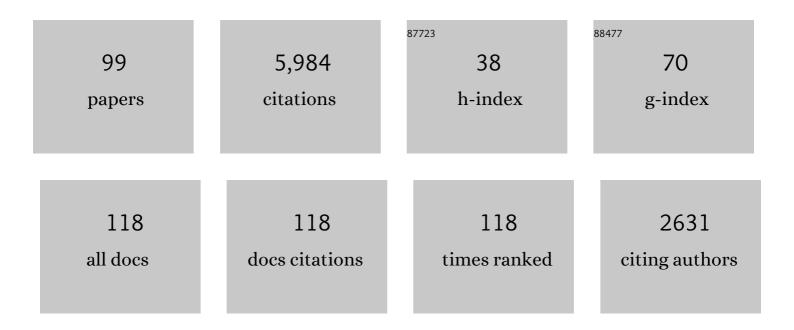
James Russell

List of Publications by Year in descending order

Source: https://exaly.com/author-pdf/4710737/publications.pdf Version: 2024-02-01



IMMES RUSSELL

#	Article	IF	CITATIONS
1	Overview of the SABER experiment and preliminary calibration results. , 1999, 3756, 277.		450
2	Validation of the Aura Microwave Limb Sounder temperature and geopotential height measurements. Journal of Geophysical Research, 2008, 113, .	3.3	370
3	Assessment of the quality of the Version 1.07 temperatureâ€versusâ€pressure profiles of the middle atmosphere from TIMED/SABER. Journal of Geophysical Research, 2008, 113, .	3.3	369
4	Retrieval of mesospheric and lower thermospheric kinetic temperature from measurements of CO215 µm Earth Limb Emission under non-LTE conditions. Geophysical Research Letters, 2001, 28, 1391-1394.	1.5	241
5	Stratospheric effects of energetic particle precipitation in 2003–2004. Geophysical Research Letters, 2005, 32, .	1.5	227
6	Evidence for slowdown in stratospheric ozone loss: First stage of ozone recovery. Journal of Geophysical Research, 2003, 108, .	3.3	224
7	Implications for atmospheric dynamics derived from global observations of gravity wave momentum flux in stratosphere and mesosphere. Journal of Geophysical Research, 2011, 116, .	3.3	203
8	The evolution of the stratopause during the 2006 major warming: Satellite data and assimilated meteorological analyses. Journal of Geophysical Research, 2008, 113, .	3.3	199
9	Energetic particle precipitation effects on the Southern Hemisphere stratosphere in 1992–2005. Journal of Geophysical Research, 2007, 112, .	3.3	186
10	The Aeronomy of Ice in the Mesosphere (AIM) mission: Overview and early science results. Journal of Atmospheric and Solar-Terrestrial Physics, 2009, 71, 289-299.	0.6	179
11	SABER observations of mesospheric temperatures and comparisons with falling sphere measurements taken during the 2002 summer MaCWAVE campaign. Geophysical Research Letters, 2004, 31, .	1.5	174
12	Severe chemical ozone loss in the Arctic during the winter of 1995–96. Nature, 1997, 389, 709-712.	13.7	155
13	The solar occultation for ice experiment. Journal of Atmospheric and Solar-Terrestrial Physics, 2009, 71, 300-315.	0.6	123
14	Global ray tracing simulations of the SABER gravity wave climatology. Journal of Geophysical Research, 2009, 114, .	3.3	120
15	Recent Northern Hemisphere stratospheric HCl increase due to atmospheric circulation changes. Nature, 2014, 515, 104-107.	13.7	110
16	Interaction of gravity waves with the QBO: A satellite perspective. Journal of Geophysical Research D: Atmospheres, 2014, 119, 2329-2355.	1.2	109
17	Atomic oxygen in the mesosphere and lower thermosphere derived from SABER: Algorithm theoretical basis and measurement uncertainty. Journal of Geophysical Research D: Atmospheres, 2013, 118, 5724-5735.	1.2	101
18	Errors in Sounding of the Atmosphere using Broadband Emission Radiometry (SABER) kinetic temperature caused by nonâ€localâ€thermodynamicâ€equilibrium model parameters. Journal of Geophysical Research, 2008, 113, .	3.3	99

#	Article	IF	CITATIONS
19	Ground-based assessment of the bias and long-term stability of 14 limb and occultation ozone profile data records. Atmospheric Measurement Techniques, 2016, 9, 2497-2534.	1.2	92
20	Interpretation of SOFIE PMC measurements: Cloud identification and derivation of mass density, particle shape, and particle size. Journal of Atmospheric and Solar-Terrestrial Physics, 2009, 71, 316-330.	0.6	91
21	GRACILE: a comprehensive climatology of atmospheric gravity wave parameters based on satellite limb soundings. Earth System Science Data, 2018, 10, 857-892.	3.7	91
22	Long-term trends of inorganic chlorine from ground-based infrared solar spectra: Past increases and evidence for stabilization. Journal of Geophysical Research, 2003, 108, .	3.3	86
23	Tropopause to mesopause gravity waves in August: Measurement and modeling. Journal of Atmospheric and Solar-Terrestrial Physics, 2006, 68, 1730-1751.	0.6	77
24	Mesopause structure from Thermosphere, Ionosphere, Mesosphere, Energetics, and Dynamics (TIMED)/Sounding of the Atmosphere Using Broadband Emission Radiometry (SABER) observations. Journal of Geophysical Research, 2007, 112, .	3.3	72
25	SABER temperature observations in the summer polar mesosphere and lower thermosphere: Importance of accounting for the CO2ν2quanta V–V exchange. Geophysical Research Letters, 2006, 33, .	1.5	68
26	Phase functions of polar mesospheric cloud ice as observed by the CIPS instrument on the AIM satellite. Journal of Atmospheric and Solar-Terrestrial Physics, 2009, 71, 373-380.	0.6	66
27	Satellite observations of ozone in the upper mesosphere. Journal of Geophysical Research D: Atmospheres, 2013, 118, 5803-5821.	1.2	63
28	The Seasonal and Long Term Changes in Mesospheric Water Vapor. Geophysical Research Letters, 1997, 24, 639-642.	1.5	61
29	Satellite observations of middle atmosphere gravity wave absolute momentum flux and of its vertical gradient during recent stratospheric warmings. Atmospheric Chemistry and Physics, 2016, 16, 9983-10019.	1.9	59
30	Polar mesospheric cloud structures observed from the cloud imaging and particle size experiment on the Aeronomy of Ice in the Mesosphere spacecraft: Atmospheric gravity waves as drivers for longitudinal variability in polar mesospheric cloud occurrence. Journal of Geophysical Research, 2010, 115, .	3.3	58
31	Kinetic temperature and carbon dioxide from broadband infrared limb emission measurements taken from the TIMED/SABER instrument. Advances in Space Research, 2009, 43, 15-27.	1.2	53
32	An evaluation of trends in middle atmospheric water vapor as measured by HALOE, WVMS, and POAM. Journal of Geophysical Research, 2003, 108, n/a-n/a.	3.3	51
33	Variations of global gravity waves derived from 14Âyears of SABER temperature observations. Journal of Geophysical Research D: Atmospheres, 2017, 122, 6231-6249.	1.2	50
34	Comparative study of shortâ€ŧerm diurnal tidal variability. Journal of Geophysical Research, 2007, 112, .	3.3	49
35	Updated SABER Night Atomic Oxygen and Implications for SABER Ozone and Atomic Hydrogen. Geophysical Research Letters, 2018, 45, 5735-5741.	1.5	44
36	SOFIE PMC observations during the northern summer of 2007. Journal of Atmospheric and Solar-Terrestrial Physics, 2009, 71, 331-339.	0.6	41

#	Article	IF	CITATIONS
37	Atomic hydrogen in the mesopause region derived from SABER: Algorithm theoretical basis, measurement uncertainty, and results. Journal of Geophysical Research D: Atmospheres, 2014, 119, 3516-3526.	1.2	41
38	Increasing carbon dioxide concentration in the upper atmosphere observed by SABER. Geophysical Research Letters, 2015, 42, 7194-7199.	1.5	41
39	Comparison of polar mesospheric cloud measurements from the Cloud Imaging and Particle Size experiment and the solar backscatter ultraviolet instrument in 2007. Journal of Atmospheric and Solar-Terrestrial Physics, 2009, 71, 365-372.	0.6	39
40	Validation of SABER v2.0 Operational Temperature Data With Groundâ€Based Lidars in the Mesosphere‣ower Thermosphere Region (75–105Âkm). Journal of Geophysical Research D: Atmospheres, 2018, 123, 9916-9934.	1.2	39
41	A link between variability of the semidiurnal tide and planetary waves in the opposite hemisphere. Geophysical Research Letters, 2007, 34, .	1.5	35
42	Validation of upper mesospheric and lower thermospheric temperatures measured by the Solar Occultation for Ice Experiment. Journal of Geophysical Research, 2012, 117, .	3.3	34
43	Gravity wave activity during recent stratospheric sudden warming events from SOFIE temperature measurements. Journal of Geophysical Research D: Atmospheres, 2014, 119, 8091-8103.	1.2	34
44	Intercomparison of kinetic temperature from 15 μ m CO2limb emissions and OH*(3,1) rotational temperature in nearly coincident air masses: SABER, GRIPS. Geophysical Research Letters, 2006, 33, .	1.5	32
45	An observational and theoretical study of the longitudinal variation in neutral temperature induced by aurora heating in the lower thermosphere. Journal of Geophysical Research: Space Physics, 2013, 118, 7410-7425.	0.8	32
46	Influence of El Niño‧outhern Oscillation in the mesosphere. Geophysical Research Letters, 2013, 40, 3292-3296.	1.5	32
47	Evidence for an OH(Ï) excitation mechanism of CO24.3 μm nighttime emission from SABER/TIMED measurements. Journal of Geophysical Research, 2004, 109, .	3.3	31
48	Gravity wave variations in the polar stratosphere and mesosphere from SOFIE/AIM temperature observations. Journal of Geophysical Research D: Atmospheres, 2014, 119, 7368-7381.	1.2	31
49	Validation of the global distribution of CO ₂ volume mixing ratio in the mesosphere and lower thermosphere from SABER. Journal of Geophysical Research D: Atmospheres, 2015, 120, 12,067.	1.2	31
50	Zonalâ€mean global teleconnection from 15 to 110 km derived from SABER and WACCM. Journal of Geophysical Research, 2012, 117, .	3.3	27
51	Radiative and energetic constraints on the global annual mean atomic oxygen concentration in the mesopause region. Journal of Geophysical Research D: Atmospheres, 2013, 118, 5796-5802.	1.2	26
52	A comparison of middle atmospheric water vapor as measured by WVMS, EOSâ€MLS, and HALOE. Journal of Geophysical Research, 2007, 112, .	3.3	25
53	Validation of ACE-FTS version 3.5 NO _{<i>y</i>} species profiles using correlative satellite measurements. Atmospheric Measurement Techniques, 2016, 9, 5781-5810.	1.2	25
54	Mid-latitude mesospheric clouds and their environment from SOFIE observations. Journal of Atmospheric and Solar-Terrestrial Physics, 2016, 149, 1-14.	0.6	24

#	Article	IF	CITATIONS
55	Impacts of SABER CO ₂ â€based eddy diffusion coefficients in the lower thermosphere on the ionosphere/thermosphere. Journal of Geophysical Research: Space Physics, 2016, 121, 12,080.	0.8	24
56	Southern Hemisphere Summer Mesopause Responses to El Niño–Southern Oscillation. Journal of Climate, 2016, 29, 6319-6328.	1.2	23
57	High-Latitude Gravity Wave Measurements in Noctilucent Clouds and Polar Mesospheric Clouds. , 2011, , 93-105.		23
58	Morphology of polar mesospheric clouds as seen from space. Journal of Atmospheric and Solar-Terrestrial Physics, 2013, 104, 234-243.	0.6	21
59	Concentric gravity waves in polar mesospheric clouds from the Cloud Imaging and Particle Size experiment. Journal of Geophysical Research D: Atmospheres, 2014, 119, 5115-5127.	1.2	21
60	A combined solar and geomagnetic index for thermospheric climate. Geophysical Research Letters, 2015, 42, 3677-3682.	1.5	21
61	Largeâ€Amplitude Mountain Waves in the Mesosphere Observed on 21 June 2014 During DEEPWAVE: 1. Wave Development, Scales, Momentum Fluxes, and Environmental Sensitivity. Journal of Geophysical Research D: Atmospheres, 2019, 124, 10364-10384.	1.2	21
62	Characterization of a Double Mesospheric Bore Over Europe. Journal of Geophysical Research: Space Physics, 2017, 122, 9738-9750.	0.8	20
63	On Longâ€Term SABER CO ₂ Trends and Effects Due to Nonuniform Space and Time Sampling. Journal of Geophysical Research: Space Physics, 2018, 123, 7958-7967.	0.8	20
64	Resolving the mesospheric nighttime 4.3 µm emission puzzle: comparison of the CO ₂ (<i>ν</i> _{ and OH(<i>I½</i>) emission models. Atmospheric Chemistry and Physics, 2017, 17, 9751-9760.}	3 <br 1.9	sub>)
65	Variability of the Brunt–VäÃIärequency at the OH* layer height. Atmospheric Measurement Techniques, 2017, 10, 4895-4903.	1.2	19
66	Evaluation of AIM CIPS measurements of Polar Mesospheric Clouds by comparison with SBUV data. Journal of Atmospheric and Solar-Terrestrial Physics, 2011, 73, 2065-2072.	0.6	18
67	New AIM/CIPS global observations of gravity waves near 50–55Âkm. Geophysical Research Letters, 2017, 44, 7044-7052.	1.5	18
68	Oblique propagation of monsoon gravity waves during the northern hemisphere 2007 summer. Journal of Geophysical Research D: Atmospheres, 2017, 122, 5063-5075.	1.2	17
69	Validation of stratospheric temperatures measured by Michelson Interferometer for Passive Atmospheric Sounding (MIPAS) on Envisat. Journal of Geophysical Research, 2005, 110, .	3.3	16
70	Responses of Lower Thermospheric Temperature to the 2013 St. Patrick's Day Geomagnetic Storm. Geophysical Research Letters, 2018, 45, 4656-4664.	1.5	15
71	Observations of the 7-day Kelvin Wave in the Tropical Atmosphere During the CPEA Campaign. Journal of the Meteorological Society of Japan, 2006, 84A, 259-275.	0.7	15
72	Satellite observations of stratospheric hydrogen fluoride and comparisons with SLIMCAT calculations. Atmospheric Chemistry and Physics, 2016, 16, 10501-10519.	1.9	14

#	Article	IF	CITATIONS
73	Trend differences in lower stratospheric water vapour between Boulder and the zonal mean and their role in understanding fundamental observational discrepancies. Atmospheric Chemistry and Physics, 2018, 18, 8331-8351.	1.9	14
74	The SPARC water vapour assessment II: profile-to-profile comparisons of stratospheric and lower mesospheric water vapour data sets obtained from satellites. Atmospheric Measurement Techniques, 2019, 12, 2693-2732.	1.2	13
75	Intercomparison of ILAS and HALOE ozone at high latitudes. Geophysical Research Letters, 1999, 26, 835-838.	1.5	12
76	Observations of OH airglow from ground, aircraft, and satellite: investigation of wave-like structures before a minor stratospheric warming. Atmospheric Chemistry and Physics, 2019, 19, 6401-6418.	1.9	12
77	HALOE observations of a slowdown in the rate of increase of HF in the lower mesosphere. Geophysical Research Letters, 1997, 24, 3217-3220.	1.5	11
78	Ozone and temperature decadal responses to solar variability in the mesosphere and lower thermosphere, based on measurements from SABER on TIMED. Annales Geophysicae, 2016, 34, 29-40.	0.6	11
79	Trends in the polar summer mesosphere temperature and pressure altitude from satellite observations. Journal of Atmospheric and Solar-Terrestrial Physics, 2021, 220, 105650.	0.6	11
80	Global balanced wind derived from SABER temperature and pressure observations and its validations. Earth System Science Data, 2021, 13, 5643-5661.	3.7	11
81	MAHRSI observations of nitric oxide in the mesosphere and lower thermosphere. Geophysical Research Letters, 1997, 24, 3213-3216.	1.5	10
82	Radiative constraints on the minimum atomic oxygen concentration in the mesopause region. Geophysical Research Letters, 2013, 40, 3777-3780.	1.5	10
83	Absolute concentrations of highly vibrationally excited OH(Ï = 9 + 8) in the mesopause region derived from the TIMED/SABER instrument. Geophysical Research Letters, 2013, 40, 646-650.	1.5	9
84	Validation of Solar Occultation for Ice Experiment (SOFIE) nitric oxide measurements. Atmospheric Measurement Techniques, 2019, 12, 3111-3121.	1.2	9
85	Radiometric Stability of the SABER Instrument. Earth and Space Science, 2020, 7, e2019EA001011.	1.1	9
86	Ground-based assessment of the bias and long-term stability of fourteen limb and occultation ozone profile data records. , 2016, 9, 2497-2534.		9
87	Variability of the Brunt–VäÃѬ́¤frequency at the OH ^{â^—} -airglow layer height at low and midlatitudes. Atmospheric Measurement Techniques, 2020, 13, 6067-6093.	1.2	9
88	Assessment of the quality of ACE-FTS stratospheric ozone data. Atmospheric Measurement Techniques, 2022, 15, 1233-1249.	1.2	9
89	Investigating Gravity Waves in Polar Mesospheric Clouds Using Tomographic Reconstructions of AIM Satellite Imagery. Journal of Geophysical Research: Space Physics, 2018, 123, 955-973.	0.8	8
90	Derivation of gravity wave intrinsic parameters and vertical wavelength using a single scanning OH(3-1) airglow spectrometer. Atmospheric Measurement Techniques, 2018, 11, 2937-2947.	1.2	8

#	ARTICLE	IF	CITATIONS
91	Understanding the Effects of Polar Mesospheric Clouds on the Environment of the Upper Mesosphere and Lower Thermosphere. Journal of Geophysical Research D: Atmospheres, 2018, 123, 11,705.	1.2	8
92	Investigating an Unusually Large 28â€Day Oscillation in Mesospheric Temperature Over Antarctica Using Groundâ€Based and Satellite Measurements. Journal of Geophysical Research D: Atmospheres, 2019, 124, 8576-8593.	1.2	7
93	Quasiâ€Biennial Oscillation of Shortâ€Period Planetary Waves and Polar Night Jet in Winter Antarctica Observed in SABER and MERRAâ€2 and Mechanism Study With a Quasiâ€Geostrophic Model. Geophysical Research Letters, 2019, 46, 13526-13534.	1.5	7
94	Ozone and temperature decadal responses to solar variability in the stratosphere and lower mesosphere, based on measurements from SABER on TIMED. Annales Geophysicae, 2016, 34, 801-813.	0.6	6
95	Universal power law of the gravity wave manifestation in the AIM CIPS polar mesospheric cloud images. Atmospheric Chemistry and Physics, 2018, 18, 883-899.	1.9	6
96	A case study of a thermally ducted undular mesospheric bore accompanied by ripples over the western Himalayan region. Advances in Space Research, 2021, 68, 1425-1440.	1.2	6
97	A case study of a ducted gravity wave event over northern Germany using simultaneous airglow imaging and wind-field observations. Annales Geophysicae, 2022, 40, 179-190.	0.6	4
98	Solar Cycle Response of CO 2 Over the Austral Winter Mesosphere and Lower Thermosphere Region. Journal of Geophysical Research: Space Physics, 2018, 123, 7581-7597.	0.8	2
99	Technical note: LIMS observations of lower stratospheric ozone in the southern polar springtime of 1978. Atmospheric Chemistry and Physics, 2020, 20, 3663-3668.	1.9	0